Astronomy Reports, Vol. 49, No. 5, 2005, pp. 374–389. Translated from Astronomicheskiĭ Zhurnal, Vol. 82, No. 5, 2005, pp. 420–436.

Spectral Studies with the Special Astrophysical Observatory 6 m and RATAN-600 Telescopes

V. L. Afanas'ev[1], S. N. Dodonov[1], A. V. Moiseev[1], A. G. Gorshkov[2], V. K. Konnikova[2], and M. G. Mingaliev[1]

[1] *Special Astrophysical Observatory, Russian Academy of Sciences, Nizhniĭ Arkhyz, Karachaĭ-Cherkessian Republic, 357147 Russia*

[2] *Sternberg Astronomical Institute, Universitetskiĭ pr. 13, Moscow, 119899 Russia*

Received September 17, 2004; in final form, December 3, 2004

Abstract—We present optical identifications, classifications, and radio spectra for 19 radio sources from a complete sample in flux density with declinations 10°–12°30′ (J2000) obtained with the 6-m optical telescope (4000–9000 Å) and RATAN-600 radio telescope (0.97–21.7 GHz) of the Special Astrophysical Observatory. Twelve objects with redshifts from 0.573 to 2.694 have been classified as quasars, and two objects with featureless spectra as BL Lac objects. Four objects are emission-line radio galaxies with redshifts from 0.204 to 0.311 (one also displaying absorption lines), and one object is an absorption-line galaxy with a redshift of 0.214. Radio flux densities have been obtained at six frequencies for all the sources except for two extended objects. The radio spectra of five of the sources can be separated into extended and compact components. Three objects display substantial rapid (on time scales from several days to several weeks) and long-term variability of their flux densities. © *2005 Pleiades Publishing, Inc.*

1. INTRODUCTION

We present optical and radio spectra for nineteen radio sources from a complete sample in flux density having declinations 10°–12°30′ (J2000), right ascensions 0–24^h, and $|b| > 15°$. The sample was selected from the GB6 catalog [1] and contains 153 sources with flux densities above 200 mJy at 4.85 GHz [2]. We have identifications with optical objects down to 21^m for 86% of the sources with flat spectra, $\alpha_{(3.9-7.7)} > -0.5$ ($S \propto \nu^\alpha$), and 60% of the sources with steep spectra $\alpha_{(3.9-7.7)} < -0.5$.

It is necessary to obtain the redshifts of the sample sources in preparation for constructing the corresponding quasar luminosity function. Including our new results presented here, 88% of all identified sample sources have now been classified. A substantial number of the objects had been classified earlier [3]; our own previous classifications are presented in [4, 5]. The sample has been monitored in the radio since 2000.

2. RADIO AND OPTICAL OBSERVATIONS

Optical spectra of all the objects were obtained with the 6-m telescope of the Special Astrophysical Observatory (SAO) of the Russian Academy of Sciences in 2001–2002. We used the multipurpose SCORPIO spectrograph [6] in its long-slit mode with a TK1024 CCD detector (1024×1024 pixels, readout noise 3 el.). The spectral range of the spectrograph is 3800 to 9200 Å, with the dispersion being approximately 6 Å/pixel. The effective instrumental resolution was roughly 20 Å. The spectra were processed in the standard way using software developed in the Laboratory for Spectroscopy and Photometry of the SAO.

The radio observations were carried out with the RATAN-600 telescope. Seven sources were observed as part of a monitoring program to study flux-density variability on time scales of several days to several weeks. These sources were observed daily using the North sector of the RATAN-600 during September 6–November 26, 2000 (82 days), June 5–September 10, 2001 (98 days), and June 19–September 23, 2002 (97 days).

The radio flux densities of the other sources were obtained during May 31–June 4, 2001, October 31–November 19, 2001, and June 6–10, 2002 on the North sector and during October 31–November 19, 2003 on the South sector, using the flat reflector. The 2000 and 2001 observations were carried out at 0.97, 2.3, 3.9, 7.7, 11.1, and 21.7 GHz, while 0.97 GHz was excluded from the 2002 and 2003 observations. The parameters of the detectors and beams are given in [7]. A beam-modulation regime was employed at 7.7, 11.1, and 21.7 GHz.

1063-7729/05/4905-0374$26.00

Table 1. Coordinates of the objects

Radio coordinates (J2000)		Optical–radio		R	B	Reference to survey
RA	DEC	Δ RA	Δ DEC			
$01^h\ 43^m\ 31.093^s$	12° 15′ 42.95″	-0.013^s	0.07″	19.75	20.55	JVAS
02 42 29.171	11 01 00.72	−0.006	0.57	19.55		JVAS
03 15 21.039	10 12 43.12	0.081	0.09	18.69	19.89	NVSS
04 44 12.467	10 42 47.29	0.010	−0.03	18.50	19.00	JVAS
04 48 50.413	11 27 54.39	−0.001	0.21	19.08	20.01	JVAS
04 49 07.672	11 21 28.63	−0.029	0.14	18.38	20.46	JVAS
05 09 27.457	10 11 44.59	−0.001	0.08	18.53	19.18	JVAS
05 16 46.646	10 57 54.77	−0.016	0.23	17.96	19.13	JVAS
07 49 27.385	10 57 33.12	0.002	0.16	18.87	19.59	JVAS
07 58 07.658	11 36 46.05	0.072	1.80	15.95	16.29	JVAS
09 14 19.360	10 06 38.28	0.166	2.45	18.65	20.88	NVSS
13 27 54.707	12 23 08.71	−0.010	1.09	19.44	19.78	NVSS
14 53 44.241	10 25 57.57	0.003	−0.40	19.49	20.78	JVAS
15 22 12.151	10 41 30.35	0.085	−0.35	18.01		NVSS
16 27 37.032	12 16 07.11	−0.003	0.07	18.89	19.04	JVAS
17 22 44.582	10 13 35.77	−0.005	0.26		20.94	JVAS
17 28 07.051	12 15 39.48	0.007	0.55		20.88	JVAS
23 12 10.467	12 24 03.46	−0.031	−0.64	18.90	19.10	NVSS
23 15 34.250	10 27 18.57	0.095	0.05	16.92	19.27	TEXAS

The processing of the radio data is described in [2, 8]. The calibration was carried out using observations of J1347+1217, whose angular size is substantially smaller than the horizontal cross-section of the beams at all the frequencies observed. We adopted flux densities of 6.15, 4.12, 3.23, 2.36, 1.99, and 1.46 Jy at 0.97, 2.3, 3.9, 7.7, 11.1, and 21.7 GHz, respectively, for this source.

3. RADIO AND OPTICAL COORDINATES

Columns 1 and 2 of Table 1 present the J2000 coordinates of the studied objects taken from the Jodrell Bank–VLA Astrometric Survey (JVAS) catalog at 8.4 GHz [9] or the NRAO VLA Sky Survey (NVSS) catalog at 1.4 GHz [10]. The rms errors of the JVAS coordinates σ are 0.014″, while the rms errors for the NVSS coordinates are typically 0.5″. The object J2315+1027 is a double source in the NVSS; the optical object is situated at the position corresponding to the weighted average of the coordinates of the two radio sources, close to the coordinates given in the Texas Survey at 0.365 GHz [11]. Columns 3 and 4 contain the differences between the optical coordinates from the USNO astrometric survey [12] and the radio coordinates. Columns 5 and 6 present the USNO R and B magnitudes, and column 7 gives references for the coordinates. The object J0914+1006 is a double or triple source with a total extent of no less than 30″, and the difference between its optical and NVSS coordinates is substantial.

4. RESULTS

Figures 1–4 present the optical spectra of the objects, Figs. 5, 6 the radio spectra, and Table 2 data from the optical observations. The columns present (1) the name of the object, (2) the spectral lines observed, (3) their wavelengths in the rest frame of the source and as observed, (4) the redshift, (5) the spectral class, (6) the date of the observations, and (7) the exposure time in minutes. Lines marked with

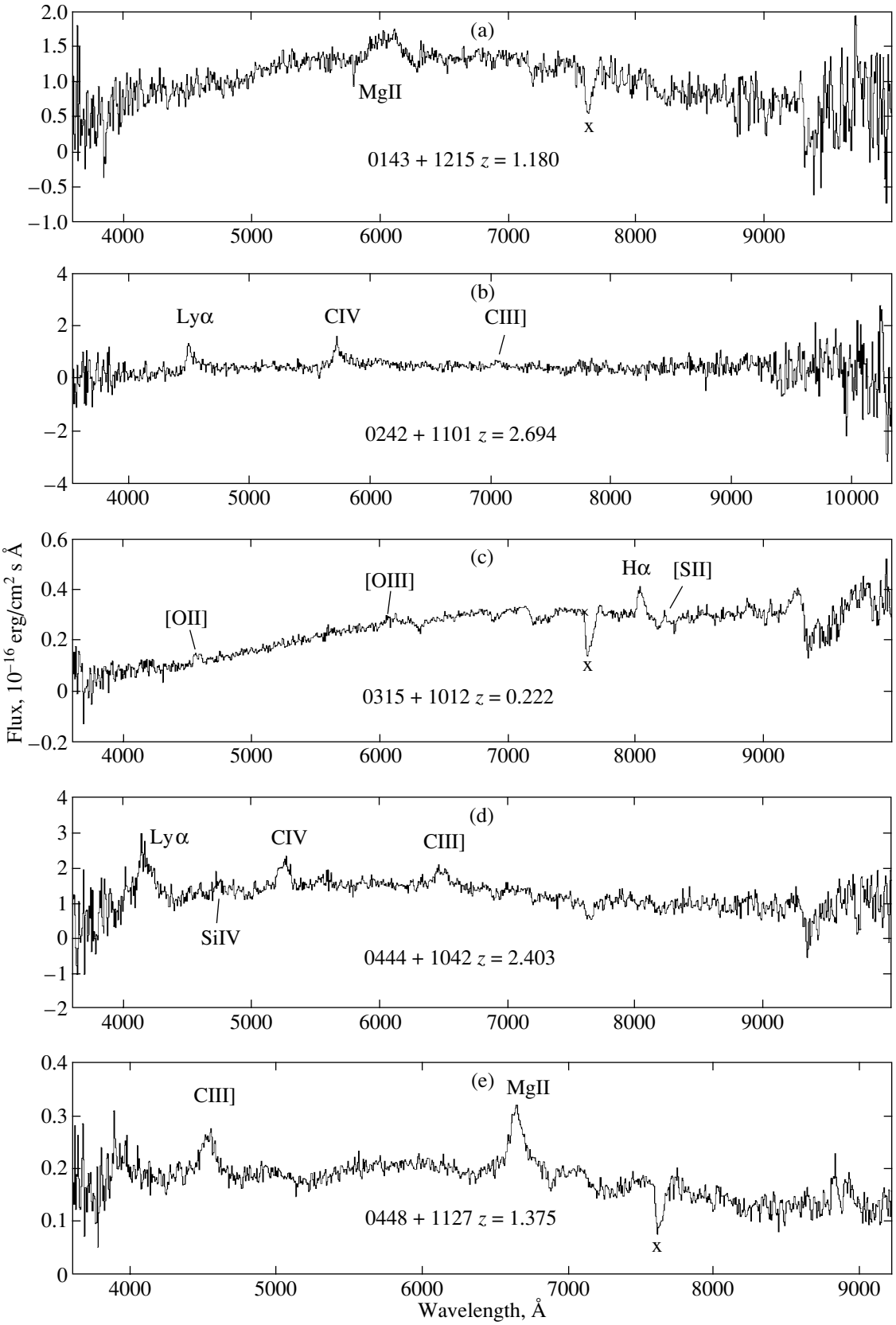

Fig. 1. Optical spectra of the radio sources J0143+1215, J0242+1101, J0315+1012, J0444+1042, and J0448+1127 obtained using the SAO 6 m telescope.

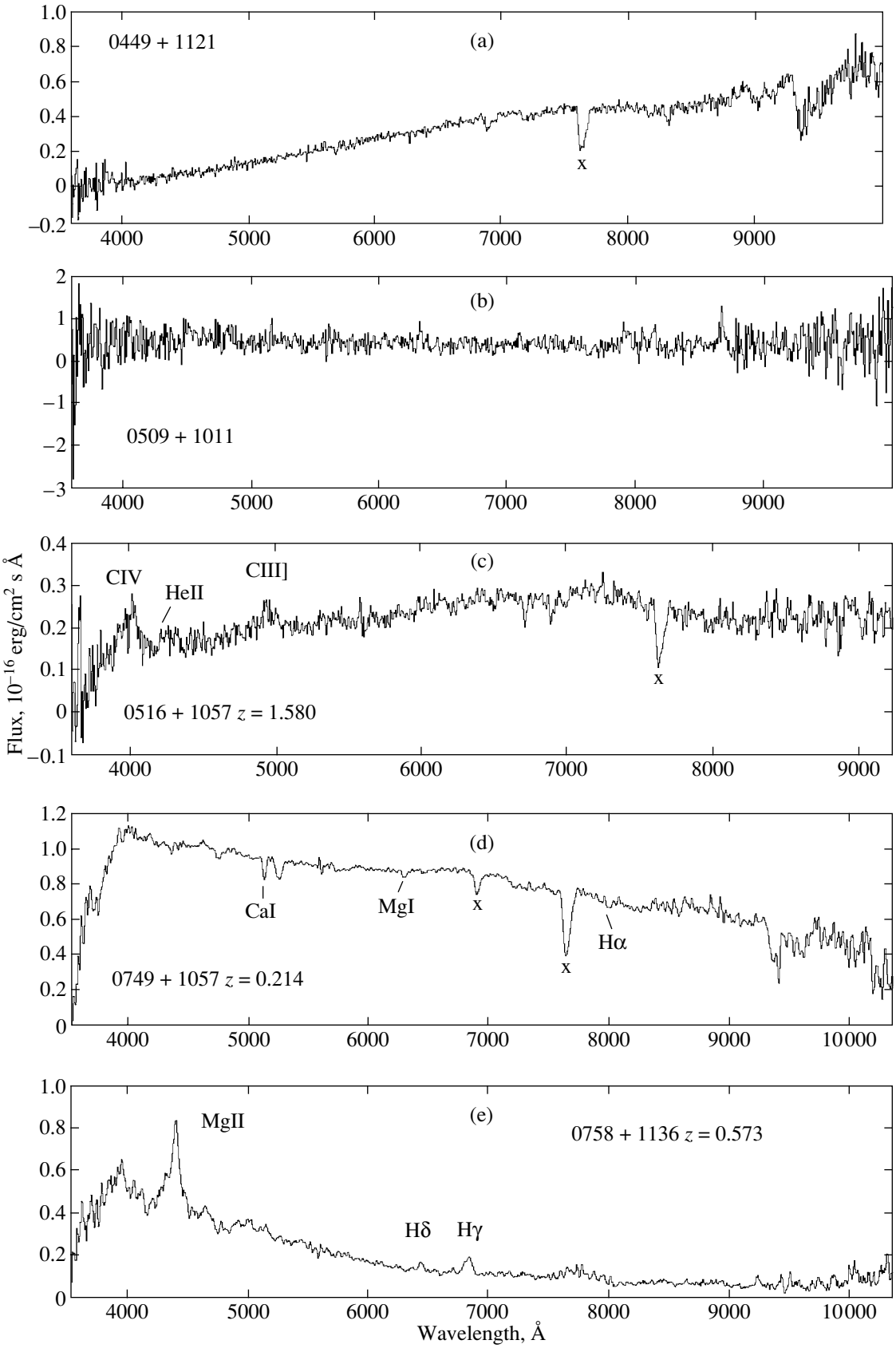

Fig. 2. Same as Fig. 1 for J0449+1121, J0509+1011, J0516+1057, J0749+1057, and J0758+1136.

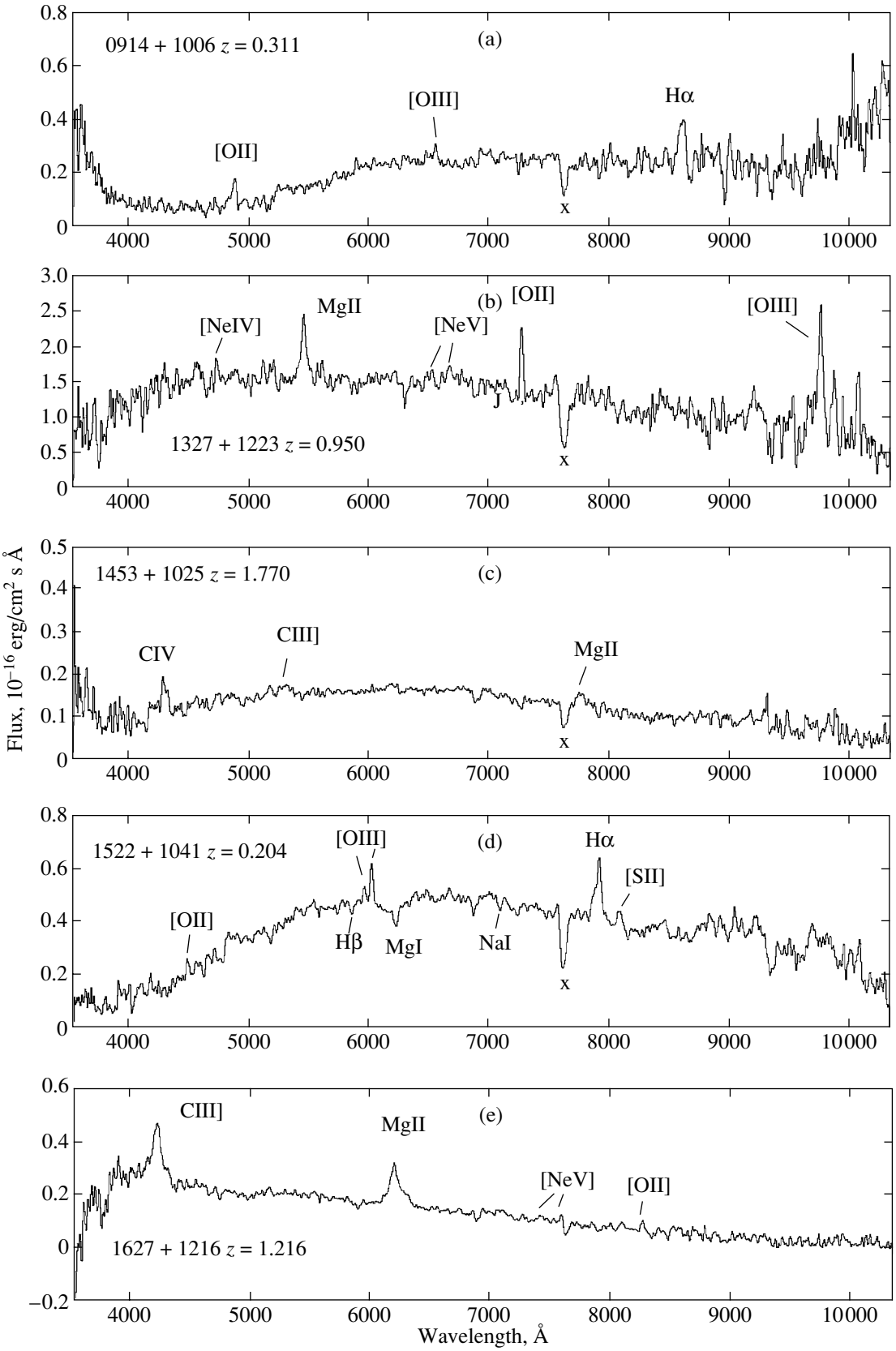

Fig. 3. Same as Fig. 1 for J0914+1006, J1327+1223, J1453+1025, J1522+1041, and J1627+1216.

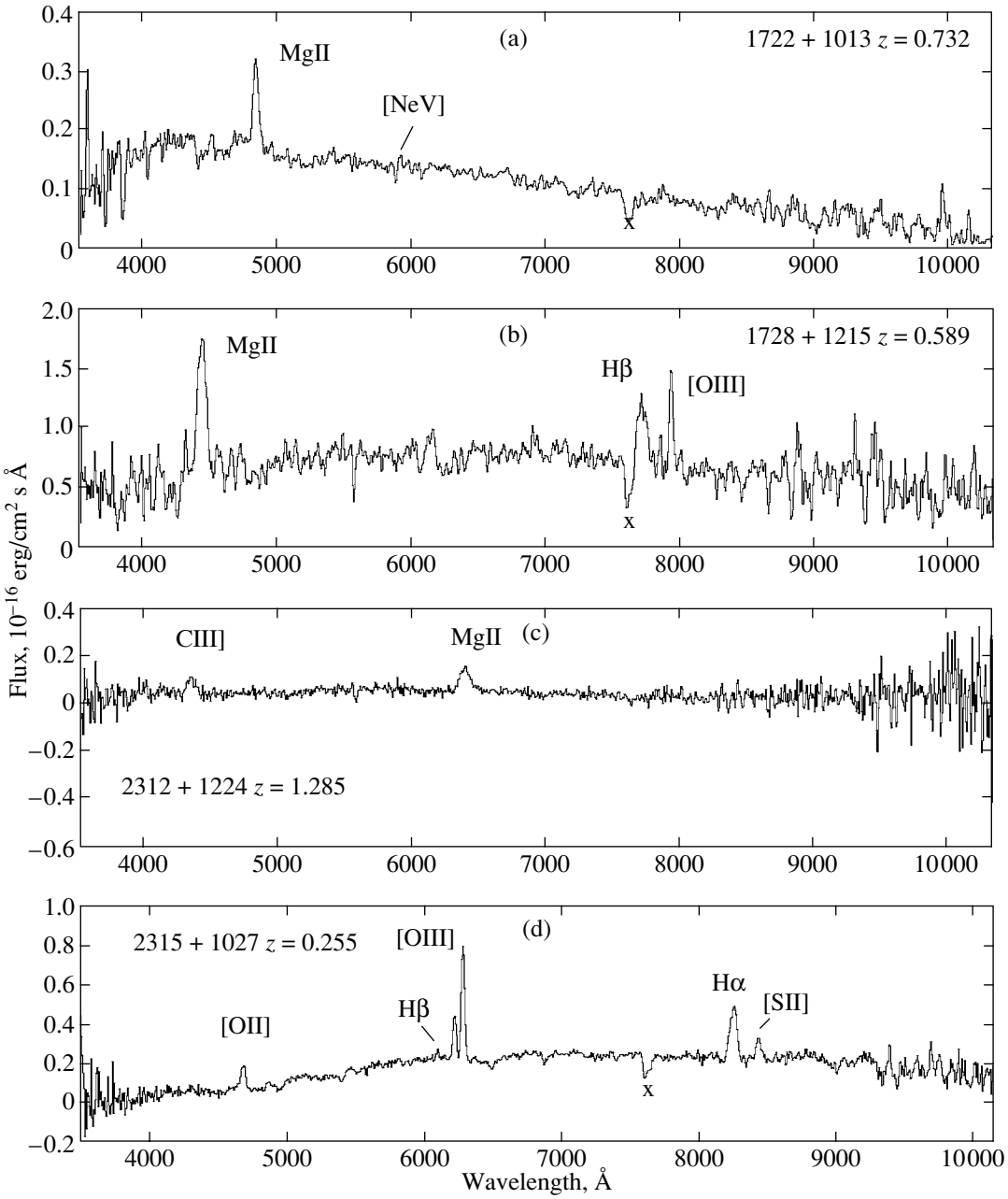

Fig. 4. Same as Fig. 1 for J1722+1013, J1728+1215, J2312+1224, and J2315+1027.

asterisks were observed in absorption, and the remaining lines in emission.

Table 3 contains the radio flux densities of the sources averaged over the observations, and presents the name of the object, the flux densities at 0.97, 2.3, 3.9, 7.7, 11.1, and 21.7 GHz in mJy and their rms errors, and the dates to which the flux densities correspond.

Observational data for variable sources are presented for multiple epochs.

Below, we discuss the optical spectrum and object classification of each object, together with the parameters of the radio spectrum.

When a non-power-law spectrum was observed, we attempted to separate it into an extended component with a power-law spectrum, $S = S_o\nu^\alpha$, and a compact component whose spectrum could be represented by a logarithmic parabola, $\log S = S_o + B\log\nu + C\log^2\nu$. The method used to separate the two components in the spectra is described in detail in [2]. This procedure also took into account the 365 MHz (Texas Survey) and 1400 MHz (NVSS) flux densities.

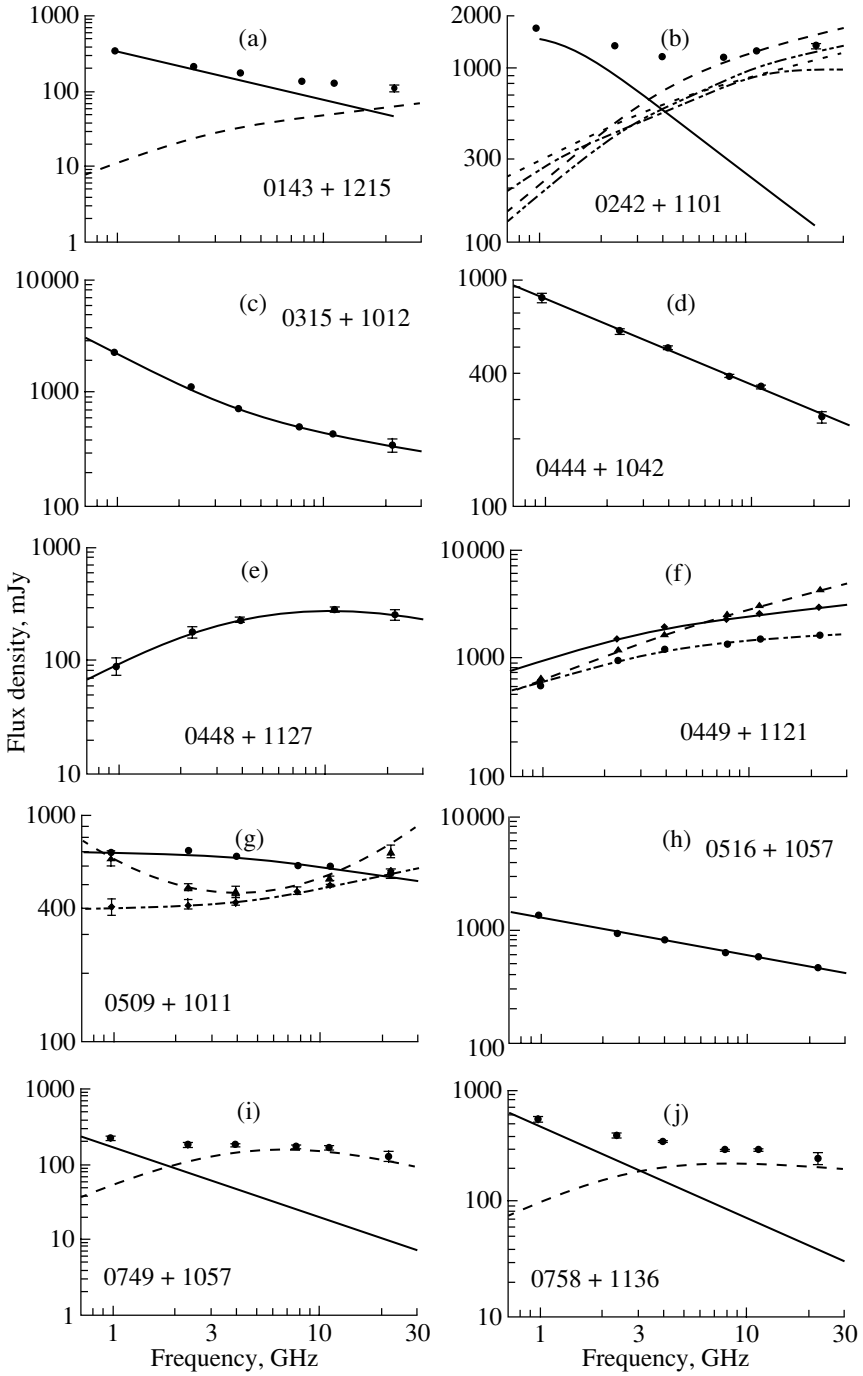

Fig. 5. Radio spectra of J0143+1215, J0242+1101, J0315+1012, J0444+1042, J0448+1127, J0449+1121, J0509+1011, J0516+1057, J0749+1057, and J0758+1136.

If the flux density of a radio source varied either from one set of observations to another or within a single set of observations, we present the parameters of the variations. For some of the sources, the relative variability amplitude is given, $V = (S_{\max} - S_{\min})/(S_{\max} + S_{\min})$. For sources with variability time scales shorter than a month, we present the modulation index m, which is defined as the ratio of the standard deviation of the variable component and the average flux density in percent.

4.1. J0143+1215

A single broad emission line is seen in the optical spectrum (Fig. 1a), interpreted as MgII 2798 Å at a redshift of $z = 1.18$. We classify this object as a

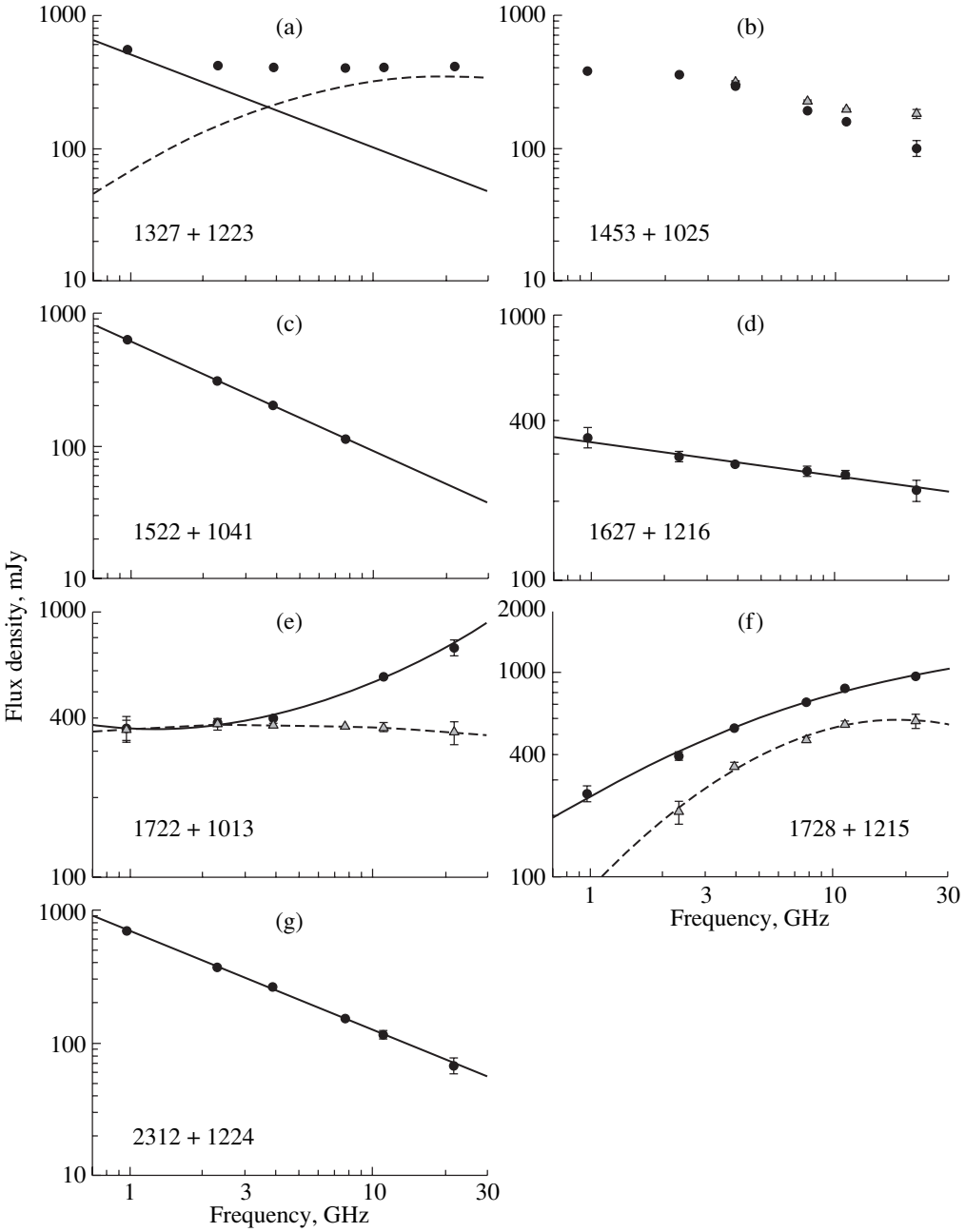

Fig. 6. Same as Fig. 5 for J1327+1223, J1453+1025, J1522+1041, J1627+1216, J1722+1013, J1728+1215, and J2312+1224.

quasar. Quasars with redshifts $z \approx 1$ usually display strong CIII] 1909 Å emission; here, however, this line is located in a noisy part of the spectrum and is not visible.

We obtained radio observations of this source in 2000, 2001, and 2002. The flux densities at all frequencies remained constant within 3σ. The spectrum falls off with frequency, flattening at high frequencies.

We were able to fit two components in the spectrum. The extended component is best fit by the power law $S = 350\,\nu^{-0.65}$ starting from 0.365 GHz. The compact component is best fit by the logarithmic parabola $\log S = 1.069 + 0.982 \log \nu - 0.322 \log^2 \nu$. The compact component is optically thick in our frequency range; the maximum flux density ($S_{\max} =$ 65 mJy) is near 35 GHz. The extended component dominates the radiation at 0.97–7.7 GHz, the flux densities of the extended and compact components are comparable at ≈13 GHz, and the radiation of the compact component begins to dominate at higher frequencies. The observed spectrum is indicated by the

Table 2. Optical data

Object	Spectral lines	Wavelength, Å	z	Spectral type	Date	Exposure time, min
J0143+1215	MgII	2798/6100	1.180	QSO	16.09.01	20
J0242+1101	Lyα	1216/4490	2.694	QSO	18.10.01	10
	CIV	1549/5720				
	CIII]	1909/7055				
J0315+1012	[OII]	3727/4550	0.222	Em. G	16.09.01	20
	Hα	6563/8020				
	[SII]	6717/8210				
J0444+1042	Lyα	1216/4140	2.403	QSO	16.09.01	16.7
	SiIV	1403/4760				
	CIV	1549/5265				
	CIII]	1909/6500				
J0448+1127	CIII]	1909/4530	1.375	QSO	15.10.01	20
	MgII	2798/6650				
J0449+1121				Lac	21.09.01	10
J0509+1011				Lac	18.10.01	10
J0516+1057	CIV	1549/4000	1.580	QSO	15.10.01	10
	HeII	1640/4215				
	CIII]	1909/4920				
J0749+1057	CaI*	4227/5130	0.214	Abs.G	15.10.01	20
	MgI*	5175/6280				
	Hα*	6563/7970				
J0758+1136	MgII	2798/4400	0.569	QSO	06.02.02	6
	Hδ	4102/6435				
	Hγ	4340/6825				
J0914+1006	[OII]	3727/4890	0.311	Em.G	06.02.02	10
	[OIII]	5007/6560				
	Hα	6563/8605				
J1327+1223	[NeIV]	2424/4725	0.950	QSO	12.05.02	10
	MgII	2798/5460				
	[NeV]	3346/6525				
	[NeV]	3426/6680				
	[OII]	3727/7270				
	[OIII]	4958/9670				
	[OIII]	5007/9760				
J1453+1025	CIV	1549/4295	1.773	QSO	08.02.02	20
	CIII]	1909/5290				
	MgII	2798/7760				

Table 2. (Contd.)

Object	Spectral lines	Wavelength, Å	z	Spectral type	Date	Exposure time, min
J1522+1041	[OII]	3727/4485	0.204	Em.G	12.05.02	10
	Hβ*	4861/5850				
	[OIII]	4958/5970				
	[OIII]	5007/6030				
	MgI*	5175/6230				
	NaI*	5893 /7095				
	Hα	6563/7903				
	[SII]	6724/8095				
J1627+1216	CIII]	1909/4228	1.216	QSO	11.05.02	10
	MgII	2798/6200				
	[NeV]	3426/7592				
	[OII]	3727/8260				
J1722+1013	MgII	2798/4845	0.732	QSO	11.05.02	10
	[NeV]	3426/5935				
J1728+1215	MgII	2798/4446	0.589	QSO	04.06.02	20
	Hβ	4861/7725				
	[OIII]	5006/7955				
J2312+1224	CIII]	1909/4360	1.285	QSO	18.10.01	10
	MgII	2798/6400				
J2315+1027	[OII]	3727/4680	0.255	Em.G	20.09.01	20
	Hβ	4861/6100				
	[OIII]	4958/6220				
	[OIII]	5007/6285				
	Hα	6563/8240				
	[SII]	6717/8430				

filled circles in Fig. 5a, with the sizes corresponding to the observational errors. The spectra of the extended and compact components are marked by the solid and dashed curves, respectively.

4.2. J0242+1101

We were able to identify three emission lines in the optical spectrum (Fig. 1b): Lyα 1216 Å, CIV 1549 Å, and CIII] 1909 Å. The redshift derived from these lines is 2.694. The object is a quasar. The Lyα line is usually stronger in radio quasars; the object may be a broad-absorption-line (BAL) quasar, with absorption in the vicinity of the nucleus partially weakening the line emission. This is also suggested by the asymmetry of the Lyα and CIV lines.

Radio observations were obtained four times in 2000–2003. All of the spectra display a minimum in the range from 3 GHz (2002) to 7.5 GHz (2000). The largest flux-density variation was detected at 21.7 GHz, from 1157 ± 15 in October 2000 to 1735 ± 20 in August 2002.

We were able to fit two components in the observed spectra. The strong extended component is best fit by the power law $S = 1930\,\nu^{-0.89}$ at 2.3–21.7 GHz; the parameters of this spectrum remained essentially constant at all observing epochs. The spectrum becomes self-absorbed at lower frequencies, with the

Table 3. Radio data

Object	Flux density with its error, mJy												Epoch
	0.97 GHz		2.3 GHz		3.9 GHz		7.7 GHz		11.1 GHz		21.7 GHz		
J0143+1215	348	10	220	06	175	03	136	04	128	02	110	10	23.07.2001
J0242+1101	1737	35	1383	17	1202	07	1082	09	1144	06	1157	15	16.10.2000
	1660	28	1340	08	1170	04	1167	06	1265	05	1378	22	23.07.2001
			1380	10	1301	04	1380	07	1507	10	1735	20	06.08.2002
			1372	40	1201	10	1106	09	1185	10	1270	50	12.09.2003
J0315+1012	2180	25	1120	20	725	08	491	09	427	14	350	45	15.11.2001
J0444+1042	820	32	596	18	500	13	377	05	340	08	250	30	15.11.2001
J0448+1127	92	15	178	15	230	11			280	11	260	20	04.11.2001
J0449+1121	430	30	1070	15	1324	19	1461	97	1654	78	1788	08	16.10.8000
	687	18	1285	10	1739	99	2671	20	3236	25	4429	34	03.07.2001
			1603	11	2035	19	2463	18	2807	72	3130	30	16.08.7001
			6871	38	1898	13	1595	13	2324	13	2782	61	12.09.2073
J0509+1011	676	18	695	16	662	08	598	05	597	01	547	15	16.10.2000
	682	11	558	10	464	04	437	05	488	01	661	21	23.02.2001
	394	52	205	20	418	14	467	17	697	08	560	35	15.11.2001
			982	26	650	05	401	08	980	08	646	08	12.09.2003
J0516+1057	1330	20	940	12	820	05	652	04	587	04	490	12	23.07.2001
			1007	30	877	07	578	06	481	12	370	35	12.09.2003
J0749+1057	219	25	180	15	182	04	169	09	165	11	126	15	04.11.2001
J0758+1136	557	30	393	20	346	05	298	07	294	07	250	20	04.11.2001
J0914+1006	420	30	260	23									02.06.2001
J1327+1223	560	30	420	15	411	09	405	10	409	08	415	20	02.06.2001
			399	45	254	15	285	10	314	14	403	40	06.09.2003
J1453+1025	383	15	359	07	293	04	194	04	160	03	116	13	23.07.2001
			353	07	321	03	230	03	198	03	184	14	06.08.2002
J1522+1041			320	14	205	10	112	06	85	17			08.06.2002
J1627+1216	348	30	294	13	275	07	259	11	252	07	220	20	15.11.2001
J1722+1013	360	30	384	12	385	07			567	07	730	48	02.06.2001
	360	25	378	18	374	07	370	06	369	12	351	34	04.11.2001
			339	30	340	06	374	06	395	07	435	32	12.09.2003
J1728+1215	257	22	394	16	537	04	716	09	849	14	960	22	16.10.2000
	250	19	403	07	524	06	613	07	737	10	793	20	23.07.2001
			316	24	429	06	517	10	578	20	571	45	08.06.2002
			210	29	350	15	470	13	565	14	584	40	12.09.2003
J2312+1224	700	25	370	15	265	11	152	05	115	07	67	09	04.11.2001

turnover frequency being near 0.7 GHz and the flux density at the turnover being $S_{\max} \approx 1600$ mJy. The extended component is plotted by the solid curve in Fig. 5b. The filled circles mark the spectrum obtained in July 2001.

In each of the four sets of observations, the spectrum of the compact component is best fit by the logarithmic parabola derived from the data averaged over the entire period of observations for this source. These spectra are plotted by the dashed and dash–dotted curves in Fig. 5b.

The spectrum of the compact component rises toward higher frequencies, with its maximum being above 40 GHz. This component is optically thick at the frequencies of our observations. The 21.7 GHz flux density reached a minimum in 2000, increased in 2001–2002, and then decreased again in 2003 to nearly its level in 2000.

These flux-density variations cannot be explained as the development of a single isolated outburst. In the standard model for the variability [13, 14], the flux density at a certain frequency should decrease only due to the transition to the optically thin part of the spectrum, which does not occur in this case. It may be that we are observing multiple outbursts whose evolution time scales are shorter than the duration of our observations. The observed evolution of the compact component is then the result of a kind of stroboscopic effect, due to our undersampling of the variations.

The flux density also varied within each set of observations. The largest variations were observed during the 97 nightly observations in 2002: the 11.1 GHz flux density increased from 1370 mJy at the beginning of this series to 1600 mJy at the end, while the 21.7 GHz flux density varied from 1400 to 1820 mJy. On June 30, 2002, the spectrum of the compact component was best fit by the parabola $\log S = 2.300 + 1.104\log\nu - 0.360\log^2\nu$, which has its maximum at $\nu_{\max} \approx 35$ GHz. Twenty days later, this spectrum was best fit by the parabola $\log S = 2.382 + 0.938\log\nu - 0.247\log^2\nu$, whose maximum is at 80 GHz. Such spectral behavior provides evidence that we are observing the evolution of two outbursts. The first was observed on June 30, 2000, while the second was observed 20 days later, at an earlier stage in its evolution. Both outbursts are well fit by logarithmic parabolas, which suggests that only one of the outbursts dominates at each these epochs. Thus, the first outburst evolved sufficiently over 20 days that its contribution to the spectrum had become negligible by the later epoch.

The object displays a high radio luminosity, close to the maximum observed for all the sources in the complete sample: $L_{\nu=11.1\ \mathrm{GHz}} = 13 \times 10^{34}$ erg/s Hz. This luminosity is calculated for a homogeneous isotropic cosmological model with zero cosmological constant, deceleration parameter $q = 0.5$, and $H = 65\ \mathrm{km\,s^{-1}\,Mpc^{-1}}$.

4.3. J0315+1012

We identified four weak emission lines with redshift $z = 0.222$ in the optical spectrum (Fig. 1c): [OII] 3727 Å, the [OIII] 4958, 5006 Å doublet, Hα 6563 Å, and [SII] 6717 Å. The object has been classified as an emission-line galaxy.

The spectrum is a power law, $S = 2055\,\nu^{-0.723}$ mJy, at 0.178–3.9 GHz. Above 3.9 GHz, the spectrum flattens due to the appearance of a compact component (Fig. 5c), however, we were not able to obtain a good two-component fit to the spectrum.

4.4. J0444+1042

Four emission lines are observed in the optical spectrum (Fig. 1d), which we identified as Lyα 1216 Å, CIV 1549 Å, and weak SiIV 1403 Å and CIII] 1909 Å at a redshift of $z = 2.403$. The object has been classified as a quasar. As for J0242+1101, the Lyα line is weaker than is typical for radio quasars, however, the line maximum may be distorted by noise.

The spectrum for November 2001 can be fit by the power law $S = 815\,\nu^{-0.372}$ mJy at 0.97–21.7 GHz (Fig. 5d). The spectrum is flat ($\alpha > -0.5$); no flux variability is observed.

4.5. J0448+1127

We identified CIII] 1909 Å and MgII 2798 Å in the optical spectrum (Fig. 1e). The full width at half maximum (FWHM) of both lines is ≈45 Å in the rest frame of the source. The redshift indicated by these lines is $z = 1.375$; the object is a quasar.

We obtained radio observations in 2001 and 2002. No flux-density variations were seen within the errors. The extended component is absent or too weak to be detected. The spectrum of the compact component averaged over the two sets of observations is best fit by the logarithmic parabola $\log S = 1.979 + 0.902\log\nu - 0.432\log^2\nu$, which has its maximum near 10 GHz and a peak flux density of 280 mJy (Fig. 5e). We were not able to measure the flux density at 7.7 GHz, because the angular distance to the adjacent strong source J0449+1121 and the distance between the feed horns of the system are very similar (the detecting equipment operates in a beam-modulation regime at this frequency). The approximate flux density at 7.7 GHz is 274 mJy.

4.6. J0449+1121

No lines are visible in the optical spectrum, and we accordingly classified this source as a BL Lac (Fig. 2a).

We obtained radio observations in 2000–2003. Figure 5f presents the spectra obtained (the spectrum for October 2000 is shown by the dash–dotted curve, for July 2001 by the dashed curve, and for July 2002 by the solid curve).

Note the strong long-term variability of the flux density (Table 3), which is accompanied by spectral variations. The spectral maximum was at 25 GHz in October 2000, but at frequencies above the observed interval at the other epochs.

The minimum flux density was observed in October 2000 at all frequencies; the maximum flux density at 7.7–21.7 GHz was observed in July 2002 and the maximum at 2.3 GHz in September 2003. The relative variability amplitudes are $V = 0.43$, 0.33, 0.29, 0.22, and 0.28 at 21.7, 11.1, 7.7, 3.9, and 2.3 GHz, respectively. These figures represent lower limits for the relative variability amplitudes, since the observations may be subject to a "stroboscopic effect" due to the presence of long gaps in the observations.

In addition to its long-term variability, the source displays strong variability on time scales shorter than a month. Analysis of the corresponding structure functions [15, 16] indicates that the characteristic time scale for variations increases with decreasing frequency.

The variability time scale is four days at 11.1 GHz, with the modulation index averaged over all epochs being $m = 3.5\%$. The characteristic time scale at 7.7 GHz is different at different epochs, and was four days ($m = 2.5\%$), five days ($m = 4.2\%$), and eight days ($m = 4.3\%$) in 2000, 2001, and 2002, respectively. The characteristic time scale was substantially longer at 3.9 GHz: 22 days ($m = 2.9$) in 2000, 10 days ($m = 4.8$) in 2001, and 16 days ($m = 5.0$) in 2002. Flux-density variations were detected at 2.3 GHz only in 2001, when they displayed a characteristic time scale of 14 days ($m = 5.0$); there are appreciable gaps in the measurements at each of the other epochs due to high levels of industrial and environmental noise.

We believe that this variability is due to scintillation in the interstellar medium; in this case, the frequency dependence of the characteristic time scale results from the frequency dependence for the angular size. The variations of the modulation index may be determined by variations in the degree of compactness of the source.

The influence of the adjacent source J0448+1127, which lies in one of the 7.7 GHz horns of the system, is significantly smaller, since its flux density is roughly a factor of five lower.

4.7. J0509+1011

The optical spectrum does not contain any lines, leading us to classify it as a BL Lac object (Fig. 2b).

Figure 5g presents the radio spectra obtained in October 2000 (solid curve) and November 2001 (dash–dotted curve) averaged over the total time spanned by the observations, together with the spectrum obtained at the end of a long series of observations in 2001, averaged over 10 days (dashed curve). The spectrum varied during June 5–September 10, 2001, and there is no single parabolic fit that is suitable for the entire averaged dataset.

Like J0449+1121, this source displays strong long-term variability of its flux density (Table 3). The shape of the spectrum also varies markedly. For example, in 2000, the spectrum could be fit well by a parabola with its maximum near 1 GHz, while the July 2001 spectrum has a minimum at 5 GHz, and the November 2001 spectrum a minimum below 1 GHz.

The flux-density variations are particularly large at 0.97, 2.3, and 3.9 GHz, where the relative amplitudes of the variability are $V = 0.27$ (October 2000, November 2001), 0.29 (October 2000, September 2003), and 0.22 (October 2000, November 2001). The dates in parentheses indicate the epochs of maximum and minimum flux density. Since no 0.97 GHz data are available after November 2001, the real relative variability amplitude at this frequency may be even higher.

It is likely that we are undersampling the variability, and that the real variability time scale does not exceed several months. This hypothesis is supported by the 21.7 GHz flux-density variations in 2001. The flux density was initially 512 ± 15 mJy, but had increased to 700 ± 20 mJy 98 days later.

The source also displays short-timescale variability. The structure functions derived from the 2000 and 2001 observations yield a characteristic time scale of three to four days. In 2000, the modulation index was $m = 4.3$, 7.4, and 10.0%, respectively, at 7.7, 3.9, and 2.3 GHz; no variability was detected at 7.7 GHz in 2001, while the modulation index was 4.5% at both 3.9 and 2.3 GHz.

4.8. J0516+1057

We were able to identify three weak emission lines with redshift $z = 1.580$ in the optical spectrum (Fig. 2c): CIV 1549 Å, HeII 1640 Å and CIII] 1909 Å. A line badly distorted by noise is visible at 7220 Å, which, at this redshift, can be identified with MgII 2798 Å. The object is classified as a quasar.

We obtained radio observations in 2001 and 2003; no significant flux-density variations were detected. The 0.97–21.7 GHz radio spectrum is best fit with the power law $S = 1270\,\nu^{-0.322}$ mJy (Fig. 5h).

4.9. J0749+1042

We identified three absorption lines in the optical spectrum (Fig. 2d): CaI 4227 Å, MgI 5175 Å, and Hα 6563 Å. The redshift derived from these lines is $z = 0.214$. The object is an absorption galaxy.

The source was observed in the radio in June 2001 and November 2001. Its flux density did not vary during this interval.

We were able to fit an extended component with a power-law spectrum starting from 0.365 GHz in the combined spectrum (Fig. 5i, filled circles): $S = 167\,\nu^{-0.92}$ mJy (solid curve). The spectrum of the compact component is best fit by the parabola $\log S = 1.761 + 0.940\log\nu - 0.532\log^2\nu$, which has its maximum flux density (150 mJy) at 7.6 GHz (dashed curve). The extended component contributes 75% of the total flux density at 0.97 GHz.

4.10. J0758+1136

Two objects are blended in the optical spectrum. After separating their spectra, one appears to be a star. Figure 2e presents the other spectrum, in which we have identified strong MgII 2798 Å, Hδ 4102 Å, and Hγ 4340 Å at a redshift of $z = 0.569$. The oxygen absorption line at ≈7650 Å is probably partially canceled out by an emission line, which may be Hβ 4861 Å, given the redshift of the object. The MgII line FWHM is ≈40 Å in the rest frame of the source. We classified this object as a quasar.

The source was observed in the radio in September 2000, June 2001, and November 2001. During this interval, the flux density remained constant within the errors. The radio spectrum falls off with frequency, flattening toward high frequencies (Fig. 5j). The spectrum (filled circles) can be divided into a power-law extended component, $S = 440\,\nu^{-0.80}$ mJy (solid curve in Fig. 5j), and a compact component, $\log S = 2.019 + 0.646\log\nu - 0.312\log^2\nu$, which has its maximum flux density (225 mJy) at 10 GHz (dashed curve).

4.11. J0914+1006

We have identified three lines in the optical spectrum with [OII] 3727 Å, [OIII] 5007 Å, and Hα 6563 Å (Fig. 3a). The object is classified as an emission-line galaxy with a redshift of $z = 0.311$.

The source is resolved in right-ascension by the RATAN-600 beam at frequencies above 3 GHz, and flux densities were obtained only at 0.97 and 2.3 GHz (Table 3). According to our measured flux densities and published data for the flux densities at 0.365, 1.4, and 4.85 GHz, the spectrum is described by the power law $S = 420\,\nu^{-0.525}$ mJy in the interval 0.365–4.85 GHz.

4.12. J1327+1223

Seven emission lines were identified in the optical spectrum (Fig. 3b): [NeIV] 2424 Å, MgII 2798 Å, [NeV] 3346 Å and [NeV] 3426 Å, [OII] 3727 Å, weak [OIII] 4958 Å, strong [OIII] 5007 Å, and MgI 5175 Å. The object is a quasar with redshift $z = 0.950$.

We obtained radio observations in 2001 and 2003. The source displays flux-density variability and a complex spectrum. Figure 6a presents the spectrum for 2001 (filled circles). An extended component with a power-law spectrum, $S = 510\,\nu^{-0.70}$ mJy, has been fit. The extended component contributes 90% of the total flux density at 0.97 GHz. At epoch June 2, 2001, the spectrum of the compact component can be described by the parabola $\log S = 1.835 + 1.075\log\nu - 0.409\log^2\nu$, which has its maximum flux density (350 mJy) at 20 GHz (Fig. 6a, dashed curve). At epoch September 6, 2003, the spectrum of the compact component can be approximated by part of a parabola that rises toward high frequencies, with the peak being located above the studied frequency interval. It is likely that the initial phase of a new outburst was observed in 2003.

4.13. J1453+1025

Three weak lines with a redshift of $z = 1.773$ were identified in the optical spectrum (Fig. 3c): CIV 1549 Å, CIII] 1909 Å, and MgII 2798 Å. The object is classified as a quasar.

We obtained radio observations in 2001 and 2002. Figure 6b presents the radio spectra for July 2001 and August 2002. Taking into account the data at 0.365 GHz, both the spectra are consistent with a two-component model: one component had its maximum at 1 GHz and remained essentially constant over the year, while the other was variable, and can be fit with parabolas with maxima near 25 GHz in July 2001 and well above the studied interval in July 2002.

4.14. J1522+0400

Both emission and absorption lines are visible in the optical spectrum (Fig. 3d). We have identified the emission lines as [OII] 3727 Å, the [OII] 4958 Å, 5007 Å doublet, Hα 6563 Å, and [SII] 6724 Å. These lines yield a redshift of $z = 0.204$. Based on this redshift, three weak absorption lines can be identified with Hβ 4861 Å, MgI 5175 Å, and NaI 5893 Å. The object is an emission-line galaxy.

The source's radio flux density is constant. Its spectrum can be described by the power law $S = 640\,\nu^{-0.832}$ mJy at 0.365–11.1 GHz (Fig. 6c).

4.15. J1627+1216

Four emission lines were identified in the optical spectrum (Fig. 3e): CIII] 1909 Å, MgII 2798 Å, [NeV] 3426 Å, and [OII] 3727 Å lines. These lines indicate a redshift of $z = 1.216$. The object is a quasar.

We obtained radio observations on June 2001 and November 2001; the flux density remained essentially constant at all frequencies during this time. The 0.97–21.7 GHz radio spectrum can be approximated with the power law $S = 333\,\nu^{-0.125}$ mJy (Fig. 6d), but the presence of large discrepancies with the fit indicates that the spectrum is complex. We were unable to separate the spectrum into components.

4.16. J1722+1013

A strong line with a width of about 50 Å is observed in the optical spectrum (Fig. 4a), which we identified with MgII 2798 Å at a redshift of $z = 0.732$; [NeV] 3426 Å with the same redshift is also detected. A weak line is visible at 8670 Å, which corresponds to [OIII] 5007 Å at the given redshift. The object is classified as a quasar.

We obtained radio observations at three epochs in 2001 and 2003. The spectrum was flat in November 2001 (Fig. 6e, dashed curve), and increased toward high frequencies at the other epochs (Fig. 6e, June 2003; the spectrum is plotted by the solid curve). A decrease in the flux density at 21.7 GHz over five months was detected—from 730 ± 48 Jy in June 2001 to 351 ± 34 Jy in November 2001. The relative amplitude of the variability is $V = 0.35$.

4.17. J1728+1215

Three strong lines are observed in the optical spectrum (Fig. 4b), which we identified with MgII 2798 Å, Hβ 4861 Å, and the [OIII] 4958, 5007 Å doublet at a redshift of $z = 0.589$. The object is a quasar.

We obtained four sets of radio observations in 2000–2003. The structure functions indicate substantial variability of the flux density on a time scale of 12 days at 3.9, 7.7, and 11.1 GHz. Figure 6f presents the spectra for October 2000 and September 2003. In the first spectrum (solid curve), the maximum lies substantially above the studied interval ($\nu_{\max} \approx 110$ GHz); in the second (dashed curve), the maximum is at $\nu_{\max} \approx 20$ GHz. The spectra obtained in 2001 and 2002 are between these two. It appears that we observed the development of a single outburst, with the flux-density maximum being shifted toward low frequencies with time.

4.18. J2312+1224

Two weak emission lines are observed in the optical spectrum (Fig. 4c), which we identified with CIII] 1909 Å and MgII 2798 Å at a redshift of $z = 1.285$. The object is a quasar.

The source displays a power-law spectrum, $S = 695\,\nu^{-0.745}$ mJy, and constant flux densities at 0.97–21.7 GHz (Fig. 6g). The spectrum can be described with the same power-law index in the broader interval 0.178–21.7 GHz.

4.19. J2315+1027

The strongest lines in the optical spectrum (Fig. 4d) can be identified with the [OIII] 4958, 5007 Å doublet and Hα 6563 Å. In addition, [OII] 3727 Å, [SII] 6717 Å, and weak Hβ 4861 Å are visible. The redshift derived from all these lines is $z = 0.255$. The object is classified as an emission-line galaxy.

Since the radio source is known to be double and is not resolved by the RATAN-600, we were not able to obtain its radio parameters.

5. CONCLUSION

We have classified the twelve radio sources J0143+1215 ($z = 1.18$), J0242+1101 ($z = 2.694$), J0444+1042 ($z = 2.403$), J0448+1127 ($z = 1.375$), J0516+1057 ($z = 1.580$), J0758+1136 ($z = 0.569$), J1327+1223 ($z = 0.950$), J1453+1025 ($z = 1.773$), J1627+1216 ($z = 1.216$), J1722+1013 ($z = 0.732$), J1728+1215 ($z = 0.589$), and J2312+1224 ($z = 1.285$) as quasars. Their optical spectra display the standard set of lines typical for quasars at the given redshifts: Lyα 1216 Å, CIV 1549 Å, CIII] 1909 Å, and MgII 2798 Å. Weaker lines are also visible in several of the spectra: SiIV 1403 Å, [NeV] 3346, 3426 Å, Hβ 4861 Å and the [OIII] 4958, 5007 Å doublet.

We observed power-law spectra ($S \propto \nu^{\alpha}$) in only these twelve quasars; two of them—J0444+1042 and J0516+1057—display flat spectra, with $\alpha = -0.372$ and $\alpha = -0.322$, respectively. The source J2312+1224 displays a steep spectrum with $\alpha = -0.745$. The flux densities of these quasars did not vary over the course of our observations.

The spectra of the other nine quasars cannot be approximated by power laws. Five of these objects display long-term variability of their flux density, while the flux densities of four objects remained constant during the interval spanned by our observations.

We were able to obtain two-component fits with an extended component, $\log S = S_o + \alpha \log \nu$, and a compact component, $\log S = S_o + B \log \nu +$

$C \log^2 \nu$, for the spectra of the four quasars J0143+1215, J0242+1101, J0758+1136, and J1327+1223.

No lines are visible in the spectra of J0449+1121 and J0509+1011, leading us to classify them as BL Lac objects. Both display substantial long-term variability with relative variability amplitudes $V = 0.2–0.4$. In addition, both sources display appreciable variability on shorter time scales of 3–4 days for J0509+1011 and 4–20 days for J0449+1121. In the latter source, the variability time scale depends on the frequency and observing epoch.

The four objects J0315+1012 ($z = 0.222$), J0914+1006 ($z = 0.311$), J1522+1041 ($z = 0.204$), and J2315+1027 ($z = 0.255$) are emission-line galaxies. The [OII] 3727 Å, [OIII] 4958, 5007 Å, and Hα 4861 Å lines typical of emission-line galaxies are visible in all their spectra. In J1522+1041, three absorption lines with the same redshift are also seen. The radio spectra of three of these objects are power laws; the spectrum of J0315+1012 is also a power law at 0.178–3.9 GHz, but flattens at lower frequencies, possibly reflecting the presence of weak compact components.

The source J0749+1057 was identified with an absorption-line galaxy at a redshift of $z = 0.214$. The spectrum can be separated into an extended and compact component, with the radiation of the compact component dominating at 2.3–21.7 GHz. We have identified a number of other radio sources with absorption-line galaxies earlier; for example, J1306+1113 [5] and J2330+1218 [4].

ACKNOWLEDGMENTS

This work was supported by the Federal Science and Technology Program "Astronomy," the Russian Foundation for Basic Research (project no. 02-07-90247), and the Federal Science and Technology Project "Universities of Russia" (project no. UR 02.03.029).

REFERENCES

1. P. C. Gregory, W. K. Scott, K. Douglas, and J. J. Condon, Astrophys. J., Suppl. Ser. **103**, 427 (1996).
2. A. G. Gorshkov, V. K. Konnikova, and M. G. Mingaliev, Astron. Zh. **80**, 978 (2003) [Astron. Rep. **47**, 903 (2003)].
3. M. P. Veron-Cetty and P. Veron, Astron. Astrophys. **374**, 92 (2001).
4. V. Chavushyan, R. Mujica, J. R. Valdez, *et al.*, Astron. Zh. **79**, 771 (2002) [Astron. Rep. **46**, 697 (2002)].
5. V. L. Afanas'ev, S. N. Dodonov, A. V. Moiseev, *et al.*, Pis'ma Astron. Zh. **29**, 626 (2003) [Astron. Lett. **29**, 579 (2003)].
6. http://www.sao.ru/moisav/scorpio/scorpio.html.
7. A. M. Botashev, A. G. Gorshkov, V. K. Konnikova, and M. G. Mingaliev, Astron. Zh. **76**, 723 (1999) [Astron. Rep. **43**, 631 (1999)].
8. A. G. Gorshkov and O. I. Khromov, Astrofiz. Issled., Izv. Spets. Astrofiz. Obs. **14**, 15 (1981).
9. I. W. A. Browne, Mon. Not. R. Astron. Soc. **293**, 257 (1998).
10. J. J. Condon, W. D. Cotton, E. W. Greisen, *et al.*, Astron. J. **115**, 1693 (1998).
11. J. N. Douglas, Astron. J. **111**, 1945 (1996).
12. D. Monet, A. Bird, B. Canzian, *et al.*, USNO-SA1.0 (US Naval Observatory, Washington DC, 1996).
13. A. P. Marscher and W. K. Gear, Astrophys. J. **298**, 114 (1985).
14. E. Valtaoja, H. Terasranta, S. Urpo, *et al.*, Astron. Astrophys. **254**, 71 (1992).
15. J. H. Simmonetti, J. M. Cordes, and D. S. Heeschen, Astrophys. J. **296**, 46 (1985).
16. P. A. Hughes, H. D. Aller, and V. F. Aller, Astrophys. J. **396**, 469 (1992).

Translated by K. Maslennikov